A R C H I V E S O F M E T A L L U R G Y A N D M A T E R I A L S
Volume 57 2012 Issue 2
DOI: 10.2478/v10172-012-0041-4

M. KUKURYK*

ANALYSIS OF DEFORMATION AND DAMAGE EVOLUTION IN HOT ELONGATION FORGING

ANALIZA ODKSZTAŁCENIA I POWSTAWANIA PĘKNIĘĆ W PROCESIE KUCIA WYDŁUŻAJĄCEGO NA GORĄCO

The paper describes the analysis of the three-dimensional stress and strain state for the process of elongation forging of the X37CrMoV51 die steel using the finite element method. The results of simulation studies of the metal flow pattern and thermal phenomena in the hot forging process carried out in three different forging tools are reported. The results of the studies have been complemented with the prediction of the occurrence of ductile fractures during forging. The numerical analysis was performed using the DEFORM-3D program. The comparison of the theoretical study and experimental test results indicates a possibility of applying the developed model to the examination of strains and prediction of material fracturing during the hot forging of die steel.

Keywords: hot forging, damage, shaped anvils, FEM

W pracy przedstawiono analizę przestrzennego stanu odkształcenia i naprężenia dla procesu kucia wydłużającego stali narzędziowej X37CrMoV51 z wykorzystaniem metody elementów skończonych. Przedstawiono wyniki prac związanych z symulacją schematu płynięcia metalu i zjawisk cieplnych w procesie kucia na gorąco w trzech różnych narzędziach kuźniczych. Rezultaty badań uzupełniono o prognozowanie powstawania pęknięć ciągliwych podczas kucia. Analizę numeryczną wykonano z wykorzystaniem programu DEFORM 3D. Porównanie teoretycznych i eksperymentalnych rezultatów badań wskazuje na możliwość zastosowania opracowanego modelu do badania odkształceń i prognozowania pękania materiału podczas kucia stali narzędziowej na gorąco.

1. Introduction

Metal forging technology plays an important role in the manufacturing industry [1]. During the forging process, an appropriate shape and required mechanical properties are imparted to the material, which are closely related to the distribution of stresses and strains, which enables one to establish the areas of the greatest plastic strains and the locations of presumable material fractures [2]. The analysis of the strain and stress state components and their variations during the plastic shaping process enables the prediction of the behaviour of material being forged, depending on the deformation history, which provides a possibility of preliminary anticipating the internal quality of the forging in the subsequent forging stages [3]. One of the directions of studies concerning this problem include endeavours to determine the material properties and the elongation forging process parameters, which lead to a breaking of the coherence of the material and formation of fractures [4].

The results of the studies being carried out, indicate a significant effect of the strain state, strain rate, temperature, microstructure parameters and friction conditions at the material-tool contact surface on the limiting effective strain value, after exceeding of which fracture of the material occurs [5]. As a result of the studies of this problem, several criteria for the occurrence of ductile fractures have been established [6]. In the present study, after preliminary verification of selected criteria for ductile fractures occurring during the plastic shaping of material, the model proposed by Cockroft and Latham [7] is applied, which assumes the principal tensile stress as the most important parameter for the initiation of discontinuities.

A finite element-based model has been developed within this study, which enables the prediction of the distribution of deformation parameters (strain, stress and temperature) and the formation of fractures during elongation forging of the X37CrMoV51 steel in three selected types of anvils. The numerical analysis was performed

* CZĘSTOCHOWA UNIVERSITY OF TECHNOLOGY, FACULTY OF MECHANICAL ENGINEERING AND COMPUTER SCIENCE, 42-200 CZĘSTOCHOWA, 21 ARMII KRAJOWEJ STR., POLAND

using the DEFORM-3D program. The positive results of the numerical study and their experimental verification enable the practical application of computer modelling to the development of rational forging tool shapes and the determination of the optimal parameters of the elongation forging process. The outcome of such activities will be improvement in the quality of steel forgings with the capability to predict the ductile fracture of the material.

2. The mathematical model implemented in the Deform 3D program

The finite element model of the forging process has been used. The solution is based on a thermal-mechanical approach described in [8]. The fields of stresses and strains are calculated by minimizing the functional:

$$\delta\varphi = \int_V \sigma_i\ \delta\dot{\varepsilon}_i\, dV + \int_V K\dot{\varepsilon}_v\, \delta\dot{\varepsilon}_v\, dV - \int_{S_F} F_i\, \delta u_i\, dS = 0 \tag{1}$$

where: σ_i is the effective stress, $\dot{\varepsilon}_i$ the effective strain rate, u_i are velocity components, S_F the

force surface, $\dot{\varepsilon}_v$ the volumetric strain rate, V the volume of the billet, F_i the traction (frictional) stress and K is a large positive penalty constant.

The temperature field is calculated by finite element solution, with relevant boundary conditions, using the Fourier equation:

$$\nabla^T \cdot (k\,\nabla T) + \dot{q} = \rho\ c_p \frac{\partial T}{\partial t} \tag{2}$$

where: k is the conductivity, T the temperature, $\dot{q}$ the rate of heat generated due to plastic deformation, ρ the density, c_p the specific heat and t the time.

The energy balance equation, Eq. (2) is written in a weak form as follows:

$$\begin{aligned} &\int_V k\ T_{,i}\ \delta T_{,i}\, dV + \int_V \rho\, c_p\, \dot{T}\delta T\ dV - \\ &- \int_V \alpha\,(\sigma_i\,\dot{\varepsilon}_i)\delta T\ dV - \int_{S_q} q_n\, \delta T\, dS = 0 \end{aligned} \tag{3}$$

where: $q_n = k\,T_{,n} = k\,T_{,i}\,n_i$ is the boundary heat flux, α is a fraction of deformation energy that converts into heat.

The finite element method is then adapted to solve Eqs. (1) and (3) which define the thermomechanical state of a body in the thermodynamic process.

The effect of friction at the anvil-workpiece interfaces was considered to be of shear -type. The frictional shear stress f is expressed as

$$f = -m\ k\left[\frac{2}{\pi}\ \tan^{-1}\left(\frac{|V_s|}{u_0}\right)\right] t \tag{4}$$

where: m is the friction factor ($0 \leqslant m \leqslant 1$), u_0 a very small positive number as compared to V_s, V_s the velocity vector of the workpiece relative to the anvil, k the local flow stress in shear and$t$ the unit vector in the direction of V_s.

In the present study, after preliminary verification of selected criteria for ductile fractures occurring during the plastic shaping of material, the model proposed by Cockroft and Latham is taken, which assumes the principal tensile stress as the most important parameter for the initiation of discontinuities. It is assumed that the formation of a discontinuity in the material will be initiated, when a certain limiting criterion value representing the ductile fracture has been exceeded. Considering the ratio of the maximum tensile stress ($\sigma_{\max}$) to the effective stress (σ_i), Cockcroft and Latham have proposed the Normalized C&L damage value criterion:

$$\int_0^{\varepsilon_i(t)} \frac{\sigma_{\max}}{\sigma_i}\, d\varepsilon_i(t) \geqslant C \tag{5}$$

where: $\sigma_{\max}$ is the maximum principal stress, σ_i the effective stress, ε_i the effective strain and C is the critical value of integral.

FEM and experimental results will be used to determine how the shape of anvils influences on the imparted damage.

3. Investigated material and simulation procedures

The flow stress values for the X37CrMoV51 steel were taken, based on plastometric tests carried out for different values of strain and strain rate, and for a fixed range of hot plastic working temperature. The experimental tests included compression of ø30×30mm axially symmetrical specimens on a cam plastometer, type MAEKAWA – Japan, with the specimens having the following chemical composition: C- 0.38%, Mn- 0.50%, Si- 0.95%, Cr- 5.0%, Mo- 1.35%, V-0.40%. The specimens were deformed at temperatures of 1173K - 1473K and at strain rates of 0.25 – 5.5 s^{-1}. The specimens were heated up to the deformation temperature in an automatically controlled electric furnace. The total true strain, as calculated from the specimen height change, was 0.105-0.693. The obtained results allowed the determination of flow stress values, as dependent on the true strain, strain rate and temperature, which were input to the program with the aim of evaluating the best rheological model for the material being deformed ($\sigma = f(\varepsilon, \dot{\varepsilon}, T)$). Sample relationships of the flow stress during upsetting of X37CrMoV51 steel specimens versus strain and temperature, for two selected strain rates of 2.3 s^{-1} and 3.8 s^{-1}

and for three temperature values (1123K, 1223K and 1473K), are shown in Figure 1. The determined curves of $\sigma = f(\varepsilon)$ exhibit a characteristic flow stress maximum that occurs at a strain slightly higher than ε_h =0.50.

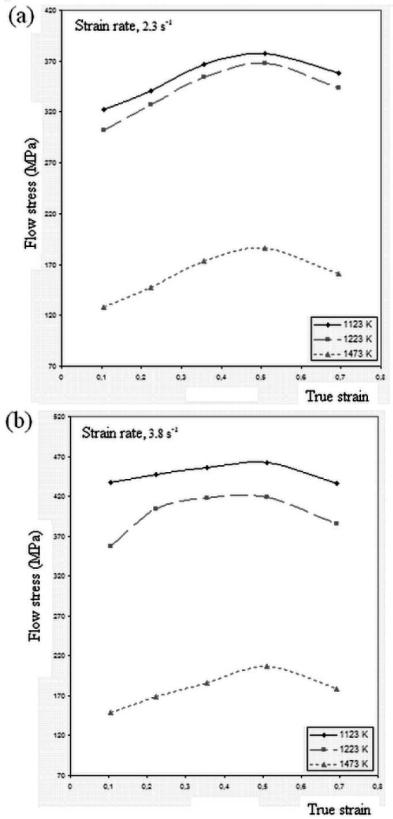

Fig. 1. Flow stress of X37CrMoV51 steel as a function of true strain and temperature, for different strain rate values, i.e.: a- $\dot{\varepsilon} = 1s^{-1}$ and b-$\dot{\varepsilon} = 2s^{-1}$

The remaining properties for steel under examination, such as density, specific heat and thermal conductivity, were assumed based on work by Kukuryk [9]. The dependence of density on temperature for steel X37CrMoV51 is described by the following relationship:

$$\rho = -2 \cdot 10^{-14}T^5 + 3 \cdot 10^{-11}T^4 - 4 \cdot 10^{-9}T^3 - \\ -3 \cdot 10^{-5}T^2 - 0.1211T + 4422.4 \tag{6}$$

The dependence of thermal conductivity on temperature for steel X37CrMoV51 is described by the relationship:

$$\lambda = -0.0001T^5 + 0.0069T^4 - 0.13443T^3 + \\ +1.057T^2 - 1.7449T + 17.213 \tag{7}$$

The dependence of specific heat on temperature for steel X37CrMoV51 is described by the relationship:

$$c_p = -0.0545T^5 + 1.6419T^4 - 17.726T^3 + \\ +86.517T^2 - 164.67T + 578.48 \tag{8}$$

In numerical computations and in experimental tests, ø80mm-diameter and 200mm-long stock of steel X37CrMoV51 was taken. The initial deformed material temperature was taken to be 1050°C, and the anvil temperature was assumed to be equal to 300°C, i.e. the anvil heating-up temperature under industrial conditions. Forging was carried out in two consecutive height reductions with tilting by an angle of 90°, while retaining a constant value of true height reduction of ε_h =0.35 and a constant relative feed of l_w =0.75. The forging was conducted in flat anvils, 135° /135° impression angle radial-rhombic anvils and in special crossed-surface anvils. The friction factor was determined on the basic of additional ring compression tests and was m =0.70 for all temperatures and all strains.

The limiting value of the normalized Cockcroft-Latham fracture criterion was determined for the X37CrMoV51 steel by a comparative method based on the notch uniaxial tensile test [10]. The limiting normalized Cockcroft-Latham fracture criterion values, as determined by the tensile test for the temperatures examined and assumed strain rates, amounted to ψ_{CL} = 0.61.

4. Results and discussion

The investigation carried out made it possible to determine the local values characterizing the strain state, the stress state and the temperature distribution, and the indices enabling the prediction of material fracturing during the elongation forging of steel X37CrMoV51 in flat anvils, 135° × 135° impression angle radial-rhombic anvils, and in special crossed-surface anvils, as shown in Figs. 2-3.

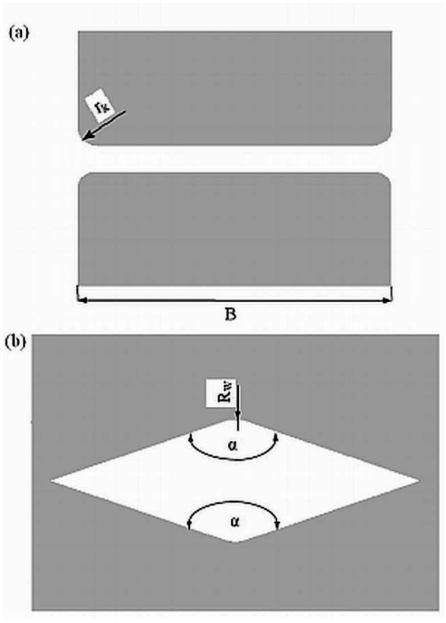

Fig. 2. Shape of anvils: a – flat ($r_k = 0.10B$), b – radial-rhombic with an impression angle of α =135°/ 135° ($R_w = 0.35D_0$)

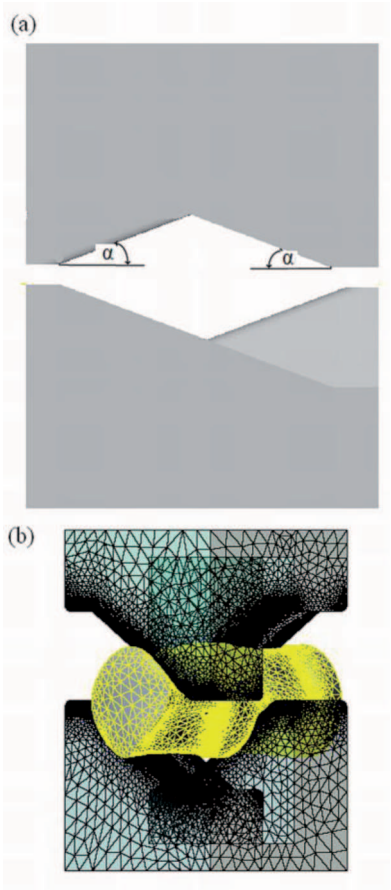

Fig. 3. The shape of the crossed – surface anvils, α =30° (a) and the view of the material deformed after the second reduction (b)

The example results of numerical computations for the 135° × 135° impression angle radial-rhombic anvils are shown in Fig. 4. The region with the maximal effective strain values lay in the immediate vicinity to the deformation zone centre and had a magnitude of $\varepsilon_i/\varepsilon_h$ =1.77 (Fig. 4a), the side zones underwent effective strain lower by two times ($\varepsilon_i/\varepsilon_h$ =0.86) and the zones situated under the die rounding tops were the regions of the lowest effective strain ($\varepsilon_i/\varepsilon_h$ =0.67). During forging in radial-rhombic anvils, no tensile stresses were found to occur in the axial forging zone (Fig. 4b).

By introducing special anvils with crossed -surfaces, a high forging reduction ($\varepsilon_i/\varepsilon_h$ =1.12) was achieved in a large part of the axial forging zone, while retaining relatively high uniformity of material forge-out (Fig. 5a). The minimal effective strain values amounted to ($\bar{\varepsilon}_i/\varepsilon_h$ =0.65). This configuration of the die working surface led to a high concentration of added non-dilatational strains in the form of thin transcrystalline layers, so called shearing micro-bands, while retaining a favourable stress state (Fig. 5b). As a result of the high plastic deformation work, the process of forging in these tools was accompanied by a considerable increase in temperature in the axial part of the material being deformed, which had a favourable influence on the thermal stability of the internal zones of forging.

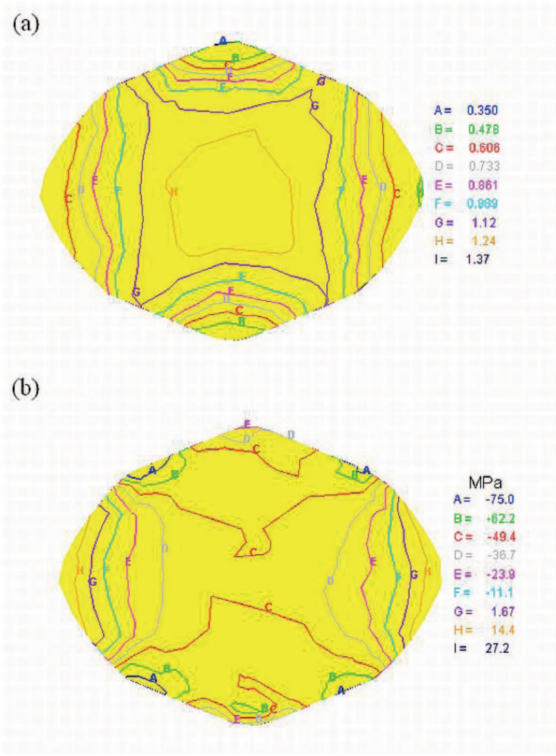

Fig. 4. Distribution of effective strain (a) and mean stress (b) after elongation forging in radial-rhombic anvils with an angle of α =135°/135° (ε_h =0.70)

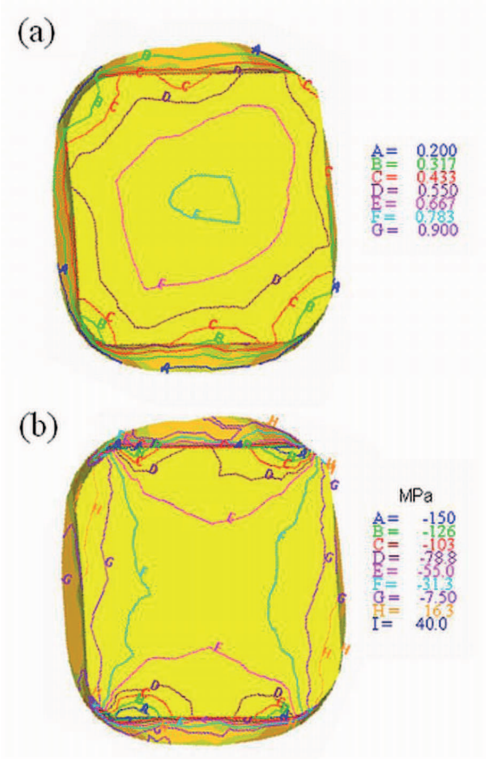

Fig. 5. Distribution of effective strain (a) and mean stress (b) after elongation forging in special crossed- surface anvils (ε_h =0.70)

The confirmation of the obtained testing results for the forging tools under examination is Fig. 6 which represents the variation of effective strain ε_i, as a function of the stress state factor k_σ, at selected points of the cross-section during forging of X37CrMoV51 steel specimen (ε_h =0.70). The greatest effective strain values, at the advantageous stress state factor value in the axial specimen part, were obtained in the 135° ×135° radial-rhombic anvils. In the special crossed-surface anvils, a relatively high and, at the same time, uniform distribution of effective strain values within a large region of the axial forging zone was obtained at the advantageous stress state factor value. The poorest results were obtained from the flat anvils.

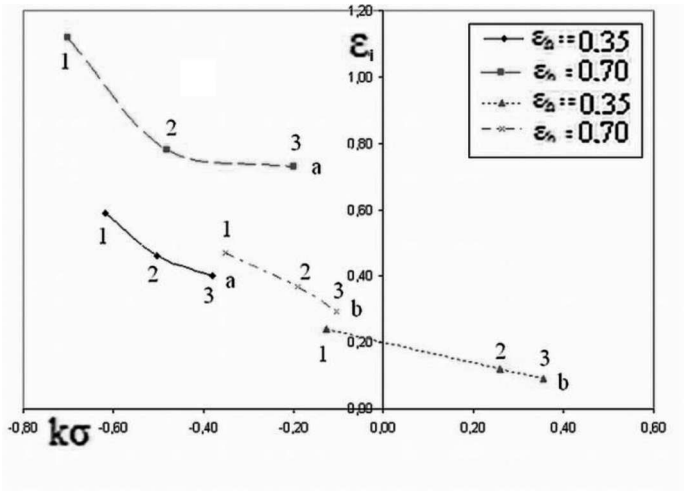

Fig. 6. The variation of effective strain ε_i as a function of the stress state factor $k_\sigma(k_\sigma = \sigma_m/\sigma_i)$ during the forging of X37CrMoV51 steel specimens in the following types of anvils: 1 – 135°/ 135° angle radial-rhombic, 2 – special crossed-surface and 3 – flat (a – deformation zone centre, b – deformed material side zone)

The represented in Figures 7 and 8 distributions of the damage factor to the Normalized Cockcroft and Latham damage value criterion (ψ_{CL}) over the cross-sectional surface of X37CrMoV51 steel specimens after elongation forging in flat anvils (Fig. 7a), 135°/135° radial-rhombic anvils (Fig. 7b), and special crossed-surface anvils (Fig. 8), show significant differences in damage factor values for particular tools. The Normalized Cockcroft and Latham damage factor in the specimen axis is definitely more advantageous than the damage factor on the specimen lateral surface, regardless of the shaped anvils. This part of the deformation zone will first attain the limiting value of the Normalized Cockcroft and Latham damage value criterion.

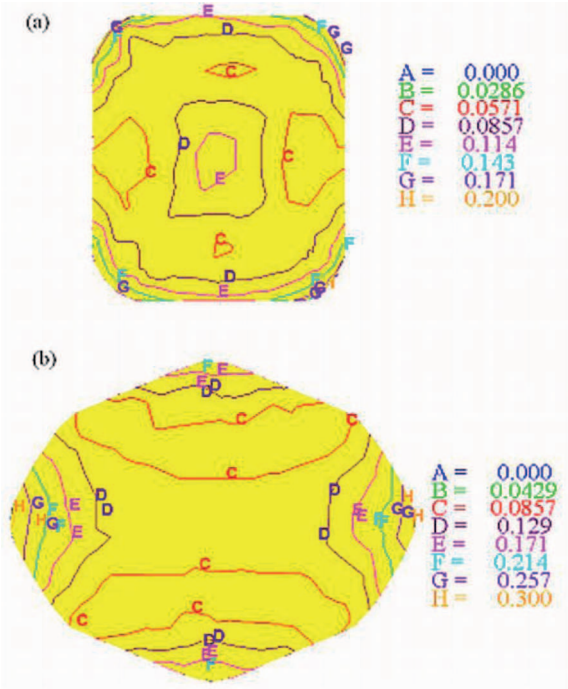

Fig. 7. Distribution of the damage factor after the elongation forging of X37CrMoV51 steel specimens in: flat anvils (a) and 135° ×135° angle radial-rhombic anvils (b), true strain ε_h = 0.70

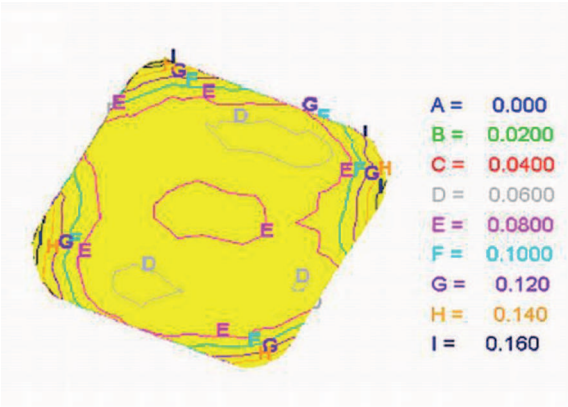

Fig. 8. Distribution of the damage factor after the elongation forging of X37CrMoV51 steel specimen in special crossed-surface anvils (ε_h = 0.70)

The twofold increase of the true reduction (ε_h =0.69) caused the proportional increase of the damage factor ψ_{CL}. The highest values of the Normalized Cockcroft and Latham damage factor were obtained during forging on flat anvils, while the highest for the 135°/135° angle radial-rhombic anvils. During one stroke of the press equipped with flat anvils, the damage factor ψ_{CL} =0.055 was obtained for the specimen axial zone, whereas for 135° /135° angle radial-rhombic dies the damage factor ψ_{CL} =0.019 was obtained. This means that the material in the axial zone can be deformed in flat anvils without breaking its coherence in 12 reductions,

while on 135°/135° angle radial-rhombic anvils in 34 reductions.

To verify the model studies, computations of the process of X37CrMoV51 steel elongation forging under industrial conditions were performed. The basic stock material in forges manufacturing heavy forgings is the forging billet. In industrial practice, the elongation forging process is carried out using flat anvils being the most universal. The input data for the thermomechanical simulation of the elongation forging process were taken from the program of forging an 8000 kg. billet on the integrated forging equipped with a 20 MN computer controlled press with two manipulators. In numerical computations and in experimental tests, ø850mm-diameter, 1500mm-long stock of the X37CrMoV51 steel was assumed. The initial material temperature was taken at 1124°C (as per the industrial forging scheme), and the initial temperature of anvils was assumed to be 300°C. Forging was carried out in flat anvils in 14 consecutive height reductions with tilting by an angle of 90°, while maintaining the following magnitudes of true strain: ε_h =0.094 (reduction 1-4), ε_h =0.139 (reduction 5-8), ε_h =0.20 (reduction 9-10) and ε_h =0.236 (reduction 11-14). A constant relative feed of l_w =0.75 was applied. During forging, the deformed material temperature was recorded after each reduction using the installed thermovision camera.

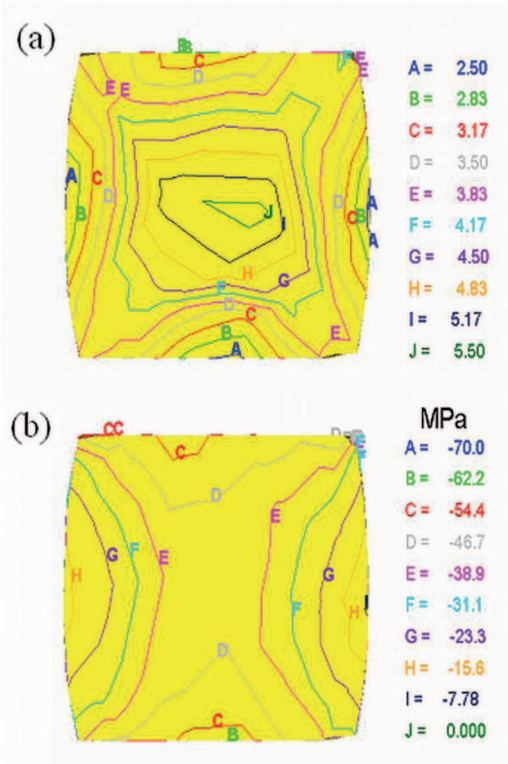

Fig. 9. Distribution of effective strain (a) and mean stress (b) on the cross-sectional surface of X37CrMoV51 steel specimens after multi-stage elongation forging in flat anvils. Forging ratio of 4.75

The analysis of strain and stress fields (Fig. 9) shows qualitative and quantitative changes in the process of billet elongation forging on flat anvils under industrial conditions. During the elongation forging of the X37CrMoV51 steel, it was found that the strain state exhibited considerable non-uniformity (Fig. 9a, $\varepsilon_{i_{\max}}/\varepsilon_{i_{\min}}$ =1.95). In the presented distribution of local strains, several characteristic zones can be distinguished. The region adjacent to the die surface undergoes small strains (ε_i = 2.83). The greatest strains occur in the middle forging part (ε_i =5.50), similarly, the side forging zones are a region of smaller strains (ε_i =2.83). The presented mean strain distribution indicates that tensile stresses can appear on the lateral surfaces of deformed material during forging (Fig. 9b).

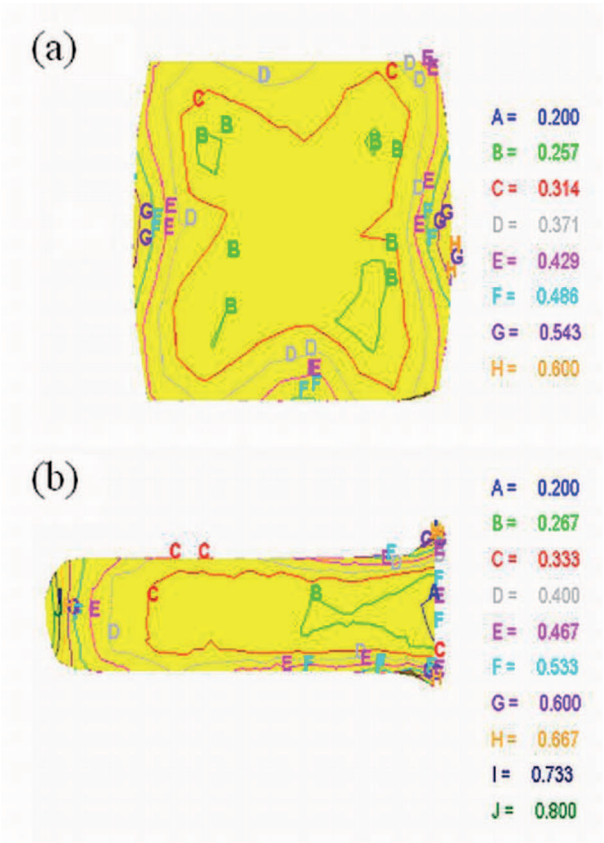

Fig. 10. Distribution of the damage factor on the surface of the cross-section (a) and longitudinal section (b) of X37CrMoV51 steel specimens after multi-stage elongation forging in flat anvils. Forging ratio of 4.75

Figure 10 shows the distributions of the damage factor to the Normalized Cockcroft and Latham damage value criterion (ψ_{CL}) on the cross-section (Fig. 10a) and longitudinal section (Fig. 10b) after the elongation forging of the X37CrMoV51 steel in flat anvils (forging ratio, K =4.75). Significant differences in the values of the damage factor ψ_{CL} in particular regions of the forging are visible on the surface of the presented sections. The

Normalized Cockcroft and Latham damage factor in the specimen axis is definitely more advantageous than the damage factor on the specimen side surface. This part of the deformation zone has first attained the limiting value of the Normalized Cockcroft and Latham damage value criterion (ψ_{CL} =0.61), for which a loss of coherence of the hot deformed metal will take place (Fig. 10b).

Figure 11 represents the damage factor ψ_{CL} as a function of true strain for two characteristic points: the forging centre (A) and the point lying on the lateral surface (B) during multi-stage forging under industrial conditions. The presented values very clearly show differences in Normalized Cockcroft and Latham damage factor values for the centre of the forging and its lateral surface. In the initial reductions, the damage factor ψ_{CL} is greater for the forging centre. In the subsequent forging phase (in reduction 4), the location of the damage factor ψ_{CL} maximum shifts from the forging centre to the side zone (p. B), and that is where, after the 14th reduction, the damage factor ψ_{CL} attains a value which is 1.5 times greater than that for the central part.

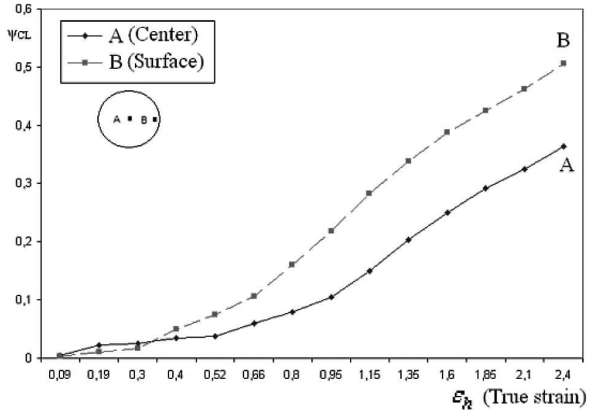

Fig. 11. Variation of the damage factor at selected points of the deformation zone during multi-stage elongation forging of X37CrMoV51 steel specimens in flat anvils. Forging ratio of 4.75

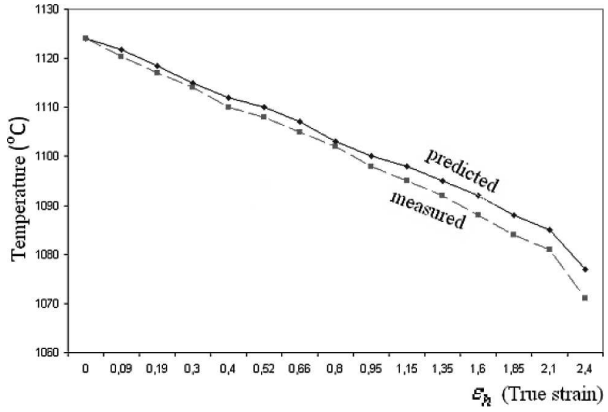

Fig. 12. Comparison of the computed temperature and the measured temperature during multi-stage elongation forging of X37CrMoV51 steel specimens in flat anvils. Forging ratio of 4.75

The computed temperature after particular reductions were juxtaposed with the experimental temperature measurement during the programmed forging of 8000 kg. billets in the integrated forging line (Fig. 12). The elongation forging process under industrial conditions is accompanied by a stable temperature in the middle forging part, and the contact between the hot metal and the cool tools causes considerable temperature gradients to occur in the vicinity of the contacting surfaces.

The experimental verification of the results of the numerical study of effective strain distribution in the flat anvils are shown in Fig. 13. The strain state has been determined using the coordination grid method. The comparative analysis of strain intensities obtained from numerical computation and experimentally has shown relatively good mutual consistence.

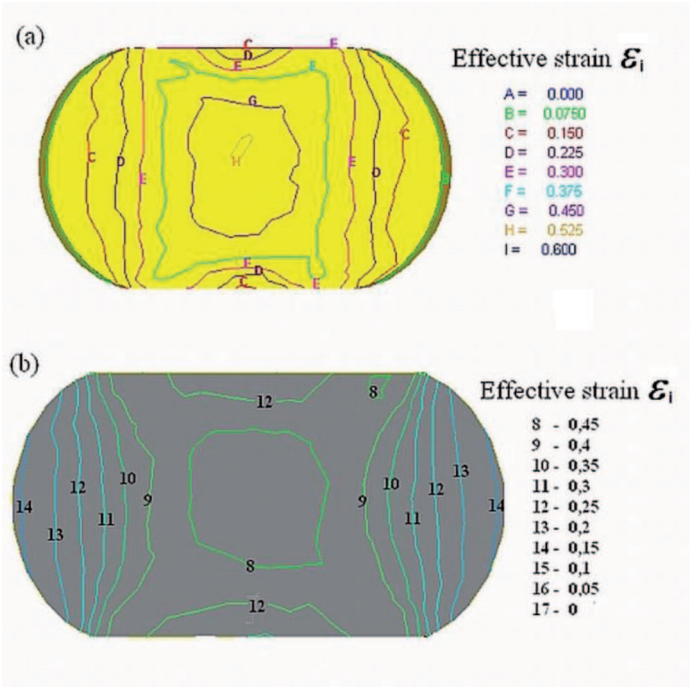

Fig. 13. Comparison of the theoretical (a) and experimental (b) distribution of effective strain on the cross-sectional surface of X37CrMoV51 steel specimens after forging in flat anvils (ε_h =0.35)

5. Conclusion

A finite element method-based three-dimensional model was employed in the research for studying the strain and stress states and predicting the damage evolution of material in the process of elongation forging of the X37CrMoV51 steel in flat and shaped anvils. The possibility of predicting the loss of coherence of the material being shaped in the forging process is an essential element of the correct design of forging technology. An important factor that changes the value of the damage

factor ψ_{CL} during elongation forging is the shape of the anvils. By the selection of the proper shapes of the forging anvils and the values of technological parameters, it is possible to significantly influence the values of the damage factor and predict the loss of coherence of the material being deformed. The variation of the damage factor to the Normalized Cockcroft and Latham damage value criterion during multi-stage elongation forging provides information on the values of the damage factor ψ_{CL} in particular deformation zones and enables the prediction of the deformation location and phase, where the loss of deformed material cohesion will take place.

The shape of the working surfaces of the crossed-surface anvils caused the formation of conditions favourable for the localization of maximal strains and concentration of considerable compressive stresses in the central part of the deformation zone. During forging on these anvils, a strong concentration of additional non-dilatational strains, so called shearing micro-bands, took place. Introducing a special crossed-surface anvil in the initial phase of elongation forging, combined with subsequent deformation in 135°/135° angle radial-rhombic anvils, will make it possible to achieve an intensive and uniform forge-out of the axial forging zone. The combination of different anvils in the elongation forging process creates possibilities for making use of their individual advantages combined.

REFERENCES

[1] S.K. Choi, M.S. Chun, C.J. Van Tyne, Y.H. Moon, Optimization of open die forging of round shapes using FEM analysis, J. Mater. Process. Technol. **172**, 88-95 (2006).

[2] T. Hatzenbichler, B. Buchmayr, A. Umgeher, A numerical sensitivity study to determine the main influence parameters on the back-end defect, J. Mater. Process. Technol. **182**, 73-78 (2007).

[3] B. Kukuryk, The analysis of the stress and strain distribution in the stretch forging process, Obróbka Plastyczna, **14**, 37-46 (2004).

[4] Q. Ma, Z. Wang, Y. Hong, The mechanism of faults originating from inclusions in the plastic deformation processes of heavy forging, J. Mater. Process. Technol. **123**, 61-66 (2002).

[5] F. Ozturk, D. Lee, Analysis of forming limits using ductile fracture criteria, J. Mater. Process. Technol. **147**, 397-404 (2004).

[6] L. Trębacz, D. Szeliga, M. Pietrzyk, Sensitivity analysis of quantitative fracture criterion based on the results of the SICO test, J. Mater. Process. Technol. **177**, 296-299 (2006).

[7] M.G. Cockcroft, D.J. Latham, Ductility and the workability of metals, Journal Institute Metals **96**, 33-39 (1968).

[8] J. Fluhrer, Deform 3D User's Manual Version 6.0, Scientific Forming Technologies Corporation, Columbus, OH (2006).

[9] M. Kukuryk, Analiza wpływu wybranych parametrów procesu kucia wydłużającego na pola naprężeń i odkształceń, Praca doktorska, Politechn. Częstochowska, Częstochowa (2010).

[10] A. Stefanik, H. Dyja, S. Mróz, Determination of the critical value of normalized Cocroft-Latham criterion during multi slight rolling based on tensile test, Archives of Metallurgy and Materials **56**, 2, 543-549 (2011).

Received: 20 December 2011.